Graphene Oxide Hybrids for Environmental Applications

Subjects: Nanoscience & Nanotechnology

Contributor: Edith Flora Joel , Galina Lujanienė

Graphene-oxide-based metal hybrids (GM) are used for the rapid and efficient reduction and removal of toxic adulterants in the environment. The exceptionally high specific surface area, versatile surface chemistry, and exceptional customization efficiency of graphene oxide nanosheets combined with the adaptable chemistry of metal nanoparticles enable the formation of GM hybrid nanocomposites. However, little is known about the architecture of GM nanocomposite engineering, interaction mechanisms, and environmental compatibility.

graphene oxide | metallic nanoparticles | gas capture | water purification | environmental | radionuclides

1. Introduction

The extraordinary optical, mechanical, electrical, and temperature characteristics of graphene make it a unique material. Recently, graphene-based nanostructures have attracted significant attention. Graphene is a honeycomb-shaped bilayer (2D) sheet of carbon particles. Other graphene structures, such as graphene oxide (GO) and reduced graphene oxide (rGO), are also being explored because of their wide range of applications in sensors, energy capacity, water sanitization, optoelectronics, and other fields. Therefore, it is important to understand the difference between GO and rGO. Graphene oxide is synthetically modified graphene. Shedding and oxidation are used to synthesize GO, which is associated with a significant adjustment of the basal plane in its structure. The monolayer GO films had a high oxygen content. The carbon/oxygen ratio of GO is often below 3:1 and close to 2:1.

Numerous investigations on the environmental applications of GO–metal-based hybrids have been published in the last decade, but the literature is replete with contradictory reports of their performance. These deviations are due in part to the highly variable nature of the synthesis methods of GM hybrid materials. The surface chemistry, lateral size, and crystalline structure of GM hybrids are predominantly dependent on the synthesis methods. Similarly, the pore size distribution and interlayer spacing can also be affected by the synthesis methods. Furthermore, half-breeds of GO/rGO with metal/metal oxide nanostructures had synergistic attributes [1].

Researchers critically review recent advances in the ecological application of GM hybrids. Most GM hybrids fabricated for water treatment are 2D and 3D materials, typically GO–metal composites, membranes, or three-dimensional matrices, in addition to a polymer. The main objective of this entry is to highlight the link between the material properties of GM hybrids and their environmental performance. Graphene has high carrier mobility,

outstanding mechanical strength and flexibility, high thermal conductivity, a large specific surface area, and excellent electrical conductivity [2]. **Figure 1** shows the graphical illustration of GM hybrids in various environmental applications.

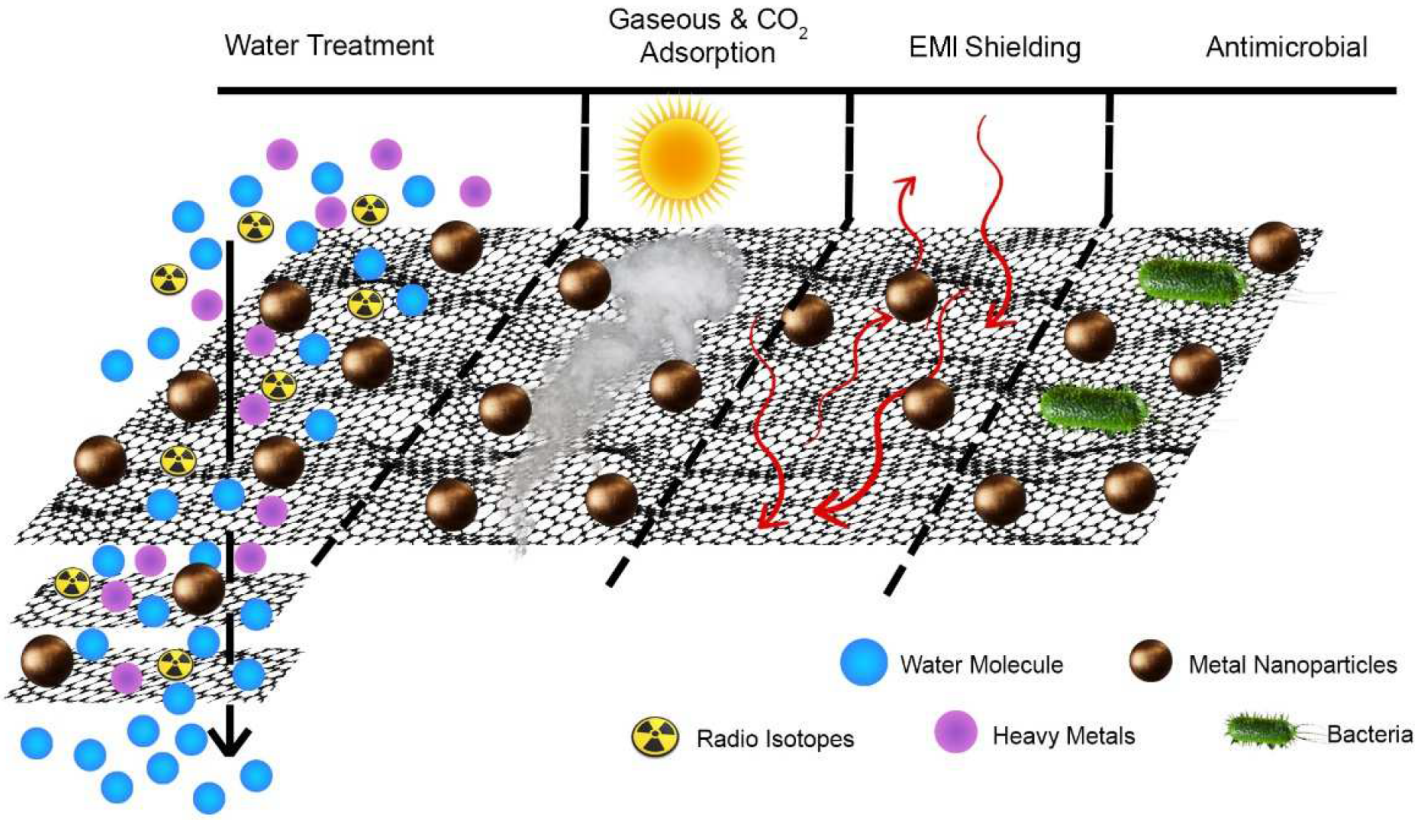

Figure 1. Schematic illustration of graphene oxide hybrids for environmental applications in water purification, gaseous CO_2 adsorption, electromagnetic shielding, and antimicrobial elimination.

2. Environmental Applications of Graphene Oxide

2.1. Water Purification

2.1.1. Removal of Heavy Metals

The toxicity of heavy metals in the environment, such as Pb, Ca, Cu, Zn, Cr, Hg, Ni, Li, Fe, As, and Cd, induces toxicity to the ecosystem. Graphene oxide and its composites are beneficial for the removal of organic pollutants and microbes from contaminated waters because of their large surface area and high catalytic efficiency. Consequently, the literature reports that the adsorption process is one of the most effective methods to remove heavy metals from the complex water matrix of the other methods available [3]. Heavy metal adsorption by graphene oxide nanocomposites involves physical adsorption [4], chemical adsorption, and electrostatic interaction [5]. The interaction of graphene oxide with heavy metals usually occurs through precipitation, ion exchange, and surface complexation. Ununiform active sites on the evacuated surface of GO promote calcium ion adsorption from hard underground water [6]. The selectivity of graphene oxide for heavy metals in a complex matrix composed of

dissolved organic matter and other contaminants was investigated by Jun et al. [7]. Negatively charged ion-chelating functional groups in GO induce nanocomposites based on graphene oxide, ideal for the removal of heavy metals, such as Cr (VI), Cu (II), Pb (II), and Cd (II), by chemical adsorption from the water matrix, as confirmed by the Langmuir model [8]. For the adequate removal of the heavy metals of greatest environmental concern in complex matrices, the limitations of graphene oxide, such as low sorption selectivity and difficulty in solid–liquid separation, can be improved by doping with metal nanoparticles. As an example, to enhance the selectivity of the heavy metal adsorption of Pb (II), graphene oxide hydrated manganese oxide nanocomposites (HMO@GO) were investigated [9]. Silver nanoparticles were produced on the GO sheets via the chemical reduction of Ag^+ ions on the GO surface. The fabricated Ag-GO was used as an adsorbent for malachite green (MG) and ethyl violet (EV) dyes, catalyst, and antibacterial agent by Hina et al. [10]. The functionalization of graphene oxide surfaces with more oxygen functional groups increased the adsorption capacity. Usually, oxygen functional groups are preferred for the removal of heavy metals because the negative surface charge of graphene oxide along with the negative surface charge of oxygen functional groups can aid in the efficient adsorption of positively charged heavy metals.

The use of magnetic materials in solid-phase extraction has received considerable attention considering the advantages arising from the inherent characteristics of magnetic particles. The choice of an appropriate magnetic adsorbent material dominates the selectivity and sensitivity of the method through hydrophobic interactions and hydrogen bonding. For example, Zahra et al. fabricated a reusable double-charged ionic liquid-modified magnetic graphene oxide (DIL-MGO) and applied it to the separation and preconcentration of Pb (II), Cd (II), Ni (II), Cu (II), and Cr (III). In addition to the higher adsorption efficiency, this compound (DIL-MGO) was also tested for the reclamation of these metals, which can add value to the reusability of the material [11]. Yue et al. synthesized self-propelled tubular motors containing an outer layer of graphene oxide and an inner layer of platinum as a catalyst that works under the influence of a magnetic field to remove lead from microchannels [12]. Subsequently, oxygen-rich functional groups allow graphene oxide to perform a secondary functionalization of GO for the preparation of hybrid nanomaterials. The formation of oxygen-containing functional groups in GO and its subsequent influence on its structure play a significant role in the adsorption and co-adsorption of polar and non-polar organics in fluid arrangements.

The higher adsorption sites in hybrids, achieved by suppressing particle aggregation and lowering the size of copper nanoparticles, explain the superior removal capabilities compared to bare particles [13]. Moreover, the structure of GO plays a significant role in providing access to active sites for the adsorption and regeneration of heavy metals. For example, Archana et al. [14] grafted NiO crystals onto graphene oxide sheets by hydrothermal treatment. The surface morphology of GO-NiO showed a substantial amount of space and surface wrinkles in a functionalized three-dimensional structure, resulting in greater accessibility to the active sites for the chemisorption of Pb (II) and Cd (II). The removal of selenium by water-dispersible magnetic graphene oxide nanocomposites was explored by You et al., 2014 [15].

2.2. Adsorption Equilibrium Parameters of Uranium Ions

The adsorption capacity increases with increasing temperature, mainly because the rate of diffusion, both internal and external, increases with increasing temperature. Uranium is an actinide element that is widely used in most nuclear reactors and is an important contributor to nuclear waste. The surface functional groups of GO-based nanoparticles are primarily responsible for their strong uranium adsorption. Because of the variety of functional groups on GO-based nanomaterials, the effect of different functional groups on uranium adsorption is unknown. Here, researchers attempt to correlate the adsorption parameters of materials with the adsorption of uranium. In general, sorption parameters provide information on the mechanisms involved in the adsorption process. Thermodynamic parameters, such as the Gibbs free energy change (ΔG), enthalpy change (ΔH), and the entropy change (ΔS), were calculated from temperature-dependent sorption data. The sorption of radionuclides onto GO-based materials is an endothermic and spontaneous process. The sorption of uranium on GO is influenced by the solution conditions, ionic strength, experimental conditions, pH, and temperature. Because of the thermodynamic parameters at different concentrations of the GO adsorbate and the U adsorbent, finding a correlation between entropy and enthalpy is not reasonable. In general, enthalpy–entropy compensation is present only when ΔG^0 is constant. Changes in Gibbs free energy and entropy were estimated based on temperature-dependent equilibrium constants.

2.3. CO_2 Capture

Graphene oxide can effectively remove gaseous contaminants in a manner similar to that of contaminant removal from water. Graphene oxide has been previously investigated for its potential in CO_2 capture and its electrochemical, thermal, or photocatalytic reduction to CO. The resulting CO, CH_3OH, CH_2O, HCOOH, and C_3H_8O were used as precursors for fuel and chemicals. Like the removal of impurities from water, GO can remove gaseous contaminants. Graphene-based materials are known for their potential in CO_2 capture and their electrochemical or photocatalytic reduction to CO.

Under powerful adsorption/desorption conditions, rGO can be used as an adsorbent for volatile organic compounds (at ppm levels) [16][17]. The adsorption capacity of graphene oxide is increased with increasing temperature, pressure, interlayer distance, and the addition of nitrogen compounds. As a most striking example, nitrogen-doped reduced graphene oxide (NRGO) exhibited the highest specificity for CO_2, with 3.81295232 ($g \cdot g^{-1}$) maximum specific absorbance of 3.81295232 $g \cdot g^{-1}$ and a specific surface area of 9916.88239 m^2/g [18].

The performance of graphene oxide can be improved by decorating it with catalytic nanomaterials [19]. Moreover, to improve the governing factors influencing the removal efficiency, surface chemistry can be improved by decorating the GO surface with reactive nanomaterials. Several metals and metal oxides exhibit excellent bandgap, electrical conductivity, and stability under experimental conditions. CO_2 capture can be greatly influenced by catalyst, catalyst carrier, and integration strategies. Different nanoparticles with catalytic properties can be used for CO_2 capture, such as copper [20].

The photocatalytic reduction of CO_2 requires several electron transfers and can produce a wide range of products depending on the precise reaction pathway adopted and the number of electrons transferred, which determine the

final oxidation state of the carbon atom. The photocatalytic reduction of CO_2 can be achieved using various metal composites. Graphene has shown potential as an effective electron acceptor and transporter for photocatalytic CO_2 reduction and reduces photogenerated charge carrier recombination. A study demonstrated the photocatalytic reduction of CO_2 in methanol (CH_3OH) and methane (CH_4) using silver chromate (Ag_2CrO_4) nanoparticles as photosensitizers and graphene oxide (GO) as cocatalysts. They concluded that, as a cocatalyst, GO assisted in charge transfer and improved CO_2 adsorption and catalytic sites [21]. TiO_2 and its photocatalytic ability to reduce CO_2 have been extensively studied. Due to its extensive 3.2 eV band gap and excellent efficient photoactivity, high stability, and low cost, graphene oxide can be used for excellent CO_2 reduction [22]. A vertically aligned TiO_2 nanostructure-wrapped GO/rGO layer were used for the photocatalytic reduction of CO_2 to CO. The unique morphology with graphene oxide as a cocatalyst combined with TiO_2 as a photocatalyst resulted in a maximum CO yield of 1348 µmol/g (**Figure 2**C) [23]. Indrajit et al. synthesized GO-Cu nanocomposites via a one-pot microwave process. The compound developed has a strong interaction between copper nanoparticles and graphene oxide, which helps to produce higher CO_2 of approximately 6.84 µmol/$g_{cat-1}h^{-1}$ for the reduction of photocatalytic CO_2 under visible-light irradiation [24] (**Figure 2**A). Solvothermal methods and subsequent photochemical deposition have been used to successfully create Ag-RGO-CdS nanocomposites. Zezhou et al. implemented Ag-RGO-CdS for the catalytic conversion of CO_2 to CO in a photocatalytic system with TEOA as a hole scavenger. As a result, 1.0 wt.%-Ag3.0 wt% RGO-CdS presents the highest photocatalytic performance of 1.61 µmol/h in comparison with bare CdS nanorods (0.21 µmol/h) (**Figure 2**B) [25]. Deerattrakul et al. synthesized Cu-Zn/reduced graphene oxide (rGO) catalysts by incipient wetness impregnation and estimated the hydrogenation of CO_2 to methanol using a fixed-bed tubular stainless-steel reactor. As a result, 424 mg_{MeOH} $g_{cat-1}h^{-1}$ of methanol was obtained at 250 °C with a loading content of 10 wt% Cu-Zn metals on rGO [26]. In general, a catalytic system requires an additional sacrificial donor for the photoreduction of CO_2, resulting in efficient fuel generation from CO_2. To overcome this, Tingting et al. synthesized nitrogen-doped graphene (Gr–CuC) for CO_2 in methanol under visible-light irradiation [27].

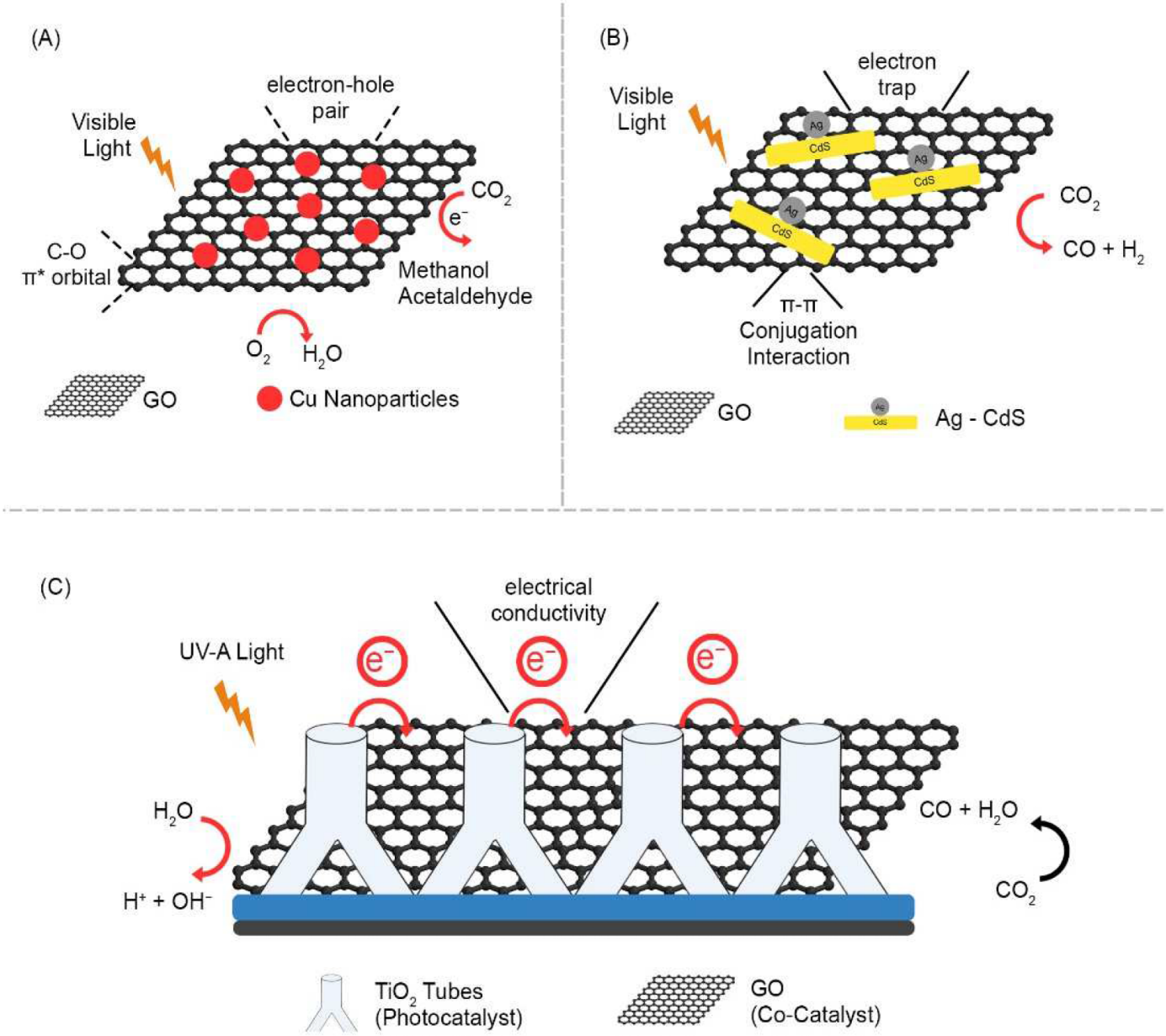

Figure 2. Mechanism of CO_2 reduction in GO metal hybrids: (**A**) Cu [24]; (**B**) Ag-Cds [25]; (**C**) TiO_2 [23].

Similarly, to minimize the overpotential of CO_2 reduction, electrocatalysts are needed in the catalytic process known as electrocatalysis, which involves reactions of oxidation and reduction by the direct transfer of electrons. The electrocatalytic CO_2 reduction reaction (CO_2RR) is an inner-sphere process in which adsorption and bond rearrangement, as well as reaction intermediates, take place inside the inner Helmholtz region (IHR). Several studies have been conducted to develop graphene oxide–metal hybrids with increased CO_2 reduction activity. Additionally, it was discovered that the rGO and CO_2 molecules interact via a π–π conjugation, which is crucial for facilitating adsorption and activating CO_2 molecules on the catalytic surface. Zhirong et al. synthesized porous In_2O_3 nanobelt-reduced graphene oxide (rGO) catalysts. To better understand the CO_2 reduction mechanism, DFT calculations were performed and compared with the experimental results. The results revealed that In_2O_3–rGO reduced CO_2 electroreduction by improving electrical conductivity and stabilizing the key intermediate $HCOO^{-*}$ [28]. Strong metal support contacts primarily contribute to improved electrochemical CO_2 reduction activity by improving

interfacial electron transfer ability, according to experimental kinetic data. Zhang et.al., used rGO supported gold nanoparticles for electro catalytic reduction of CO_2 [29]. A lone pair of nitrogen electrons interacts with transition metal complexes to form composite materials [30].

2.4. Electromagnetic Interference (EMI)

Interestingly, adaptable graphite has been utilized as an electromagnetic interference (EMI) protective material. The peeled graphite pieces were packed without fasteners to produce adaptable graphite sheets with a decent and large surface region. The EMI of adaptable graphite was estimated using the coaxial transmission technique at frequencies in the range of 1 to 2 GHz. The creators determined that the EMI SE of adaptable graphite was extremely high with this L-band recurrence. Regardless of its use for EMI safeguarding, adaptable graphite can also be utilized as an EMI gasket material because of its toughness. Given its high similarity to natural polymers, GO can be utilized as an engaging nanofiller in polymer nanocomposites, extensively developing the electrical, mechanical, and warm qualities of polymers. Furthermore, practical gatherings containing oxygen at the edges and bases of GO guide the expansion of the interfacial holding and the displacement of pressure from the polymer grid to polymer nanocomposites, resulting in polymer nanocomposites with prevalent support capacities [31]. Xu et al. synthesized large-scale thermally reduced graphene oxide films with an EMI shielding potential and high conductivity of 500 S/cm. Furthermore, the synthesized rGO sheets exhibited an excellent EMI SE of 45–54 dB, with a film thickness of less than 0.1 mm [32].

The exponential increase in the demand for electromagnetic interference shielding materials has led to the development of new shielding materials in recent years. Generally, an effective shielding material has three main functions: reflection, absorption, and multi-reflection. The high conductivity of graphene oxide (GO) makes it an ideal candidate for electromagnetic interference shielding. Multiple layers of graphene can hinder the optical transparency of a shielding material for applications in transparent films. Shi et al. proposed a cost-effective lithography technology to synthesize a four-layer graphene mesh with an even thickness. A uniform structure was achieved using an organic combination of microstructure patterning and continuous meshing. Compared to a two-layer graphene film, the four-layer graphene mesh showed a 1.26-time increase in absorption-based SE of 4.22 dB at 12–18 GHz, along with an improved transmittance efficiency of 95.26% [33]. Using adsorption as the dominant shielding mechanism, CuS/RGO compounds without any reducing agent from copper (II) dithiooxamide (Cu–DTO) and GO as a precursor were obtained via the hydrothermal method. Mechanical constancy is the priority to be assessed for the persistence of mechanical deformation in real-life applications. Using CuS as a pseudo capacitor and rGO as a conductor, a shielding efficiency of 64 dB at 2.3 GHz was achieved [34]. A novel nickel-foam-supported rGO(NI-rGO) foam was fabricated without any reducing agent. This foam is then pressed to a paper form by a hydraulic press at 20 MPa for 10 min, resulting in an RGN paper-like thin film by thermal annealing with a mechanical strain of 80% for 1000 cycles and enhanced shielding efficiency of 55 dB with 0.12 mm thickness, accompanied by a thermal conductivity of ≈247 W/(m·K) [35]. A noteworthy work by Hui Jia et al., investigated a free-standing GO/Ag nanowire (40 nm) film that covers the X-band, Ku-band, K-band, and the Ka band with an EMI shielding efficiency of 62 dB with a material thickness of 8 mm. The positively charged 1D silver nanowire with proven EMI shielding efficiency also favored the formation of the 3D conductive network via the vacuum-assisted

self-assembly route of fabrication. The GO/Ag-7L demonstrated outstanding 62 dB performance in a frequency range of 8–40 GHz. This result suggests that the Ag nanowire boosted the conduction and tunnelling in the 3D GO layer of electrons without compromising the strain value with 5000 bending cycles [36]. FeNWs-rGO Fe_3O_4 nanowires were grown on rGO sheets using an in situ growth mechanism. The authors assembled Fe_3O_4 nanowires based on spatial confinement effects into vertical, parallel, and randomly assembled Fe_3O_4 NW onto the epoxy layer via an external magnetic field. Vertically aligned Fe_3O_4 NW showed an electrical conductivity of 37 S/m and improved shielding efficiency compared to parallel and randomly assembled Fe_3O_4 NW. This is due to charge accumulation from interfacial and dipole polarization by the hetero-interfaces formed by Fe_3O_4 NW-rGO. Moreover, increased polarization relaxation and dielectric loss, assisted by the external magnetic field, attenuate the EM wave [37].

Using the dielectric loss and magnetic loss mechanism of magnetic metal nanocomposites, Zhongji et al. used a two-step approach for developing loaded iron-cobalt-nickel oxide (FeCoNiOx) onto poly-dopamine-reduced graphene oxide. The FeCoNiOx-PDA-rGO composite possessed a reflection loss value of −36.28 dB at a thickness of 6.5 mm. The reflection loss value is achieved by the dielectric loss capacity of a defective graphene surface, followed by the magnetic loss and dielectric loss mechanisms of metal and its oxides that help in the overindulgence of incident Em waves [38]. Graphene oxide for ionizing radiation was explored earlier [39][40]. Malinski et al. investigated the structural changes in irradiated GO surfaces with an energy of 40 keV using Au and GA ions and 500 keV helium and gallium ions. The irradiated GO foils were characterized by Rutherford backscattering spectrometry (RBS) and elastic recoil detection analysis (ERDA), which showed fluence of ion implantation and deoxygenation with modification of the GO surface. They also found that the modification of the elemental composition of GO after irradiation with 500 keV helium and gallium ions is due to nonelastic nuclear stopping and a low degree of GO deoxygenation [41][42].

2.5. Antimicrobial Activity

The innate antimicrobial properties of graphene oxide result from the physicochemical interactions of bacteria with oxygen-containing functional groups. This abundance of oxygen groups also assists in the hybridization of nanoparticles through electrostatic and coordinate approaches. AgNPs are known for an extensive range of antimicrobial studies against *E. coli* and *S. aureus*. Like graphene oxide, AgNPs also initiate cell death by damaging the cell membrane upon contact, producing reactive oxygen species, and interrupting ATP production. Stabilizing agents are typically used to prevent agglomeration and control its structure. Correspondingly, Mónica Cobos used an environmentally friendly approach to produce GO-AgNPs using a green reducing agent. GO-AgNPs were tested against *Escherichia coli*, *Pseudomonas aeruginosa*, and the Gram-positive bacterium *Staphylococcus aureus*. They concluded that the cytotoxicity of the nanohybrids depends on the smaller size of the silver particles, which have a larger surface area for bacterial interaction. Furthermore, nanoparticles induce dose- and time-dependent toxicity against all microorganisms, especially *C. albicans* and *S. aureus*, and were studied by Neto et al. [43].

Silver nanoparticles have gained considerable attention because of their variety of applications such as antimicrobial and medical applications over the years. Although the antibacterial property of silver nanoparticles has been exploited, the prevention of biofilms is still unclear. To test the inhibition property of biofilms on stainless-steel material (SS) used in medical procedures, Saravia et al. studied the antimicrobial property of *Pseudomonas aeruginosa* PAO 1, *Escherichia coli* (ATCC11229), *Acinetobacter* sp. (KM349193, NCBI-GenBank), *Bacillus cereus* (ATCC 10876), *Staphylococcus* sp., and *Kocuria rizophila* using the Kirby–Bauer method. *P. aeruginosa* and *K. rizophila* showed a higher sensibility towards Ag-GO nanoparticles on the SS material [44].

Moreover, the use of bimetallic nanoparticles with graphene oxide in the antibacterial field has recently been explored. Menazea et al. fabricated graphene oxide thin films decorated with silver and copper oxide nanoparticles. They prepared GO-Ag by adding $AgNO_3$ followed by NaOH to the water dispersion of GO and GO-CuO by adding $CuCl_2.2H_2O$ followed by NaOH to the water dispersion. These nanoparticles were tested against *Escherichia coli*, and *Staphylococcus aureus* showed antibacterial inhibition comparable to that of *E. coli.* Antibacterial activity was examined against both Gram-positive bacteria (*Staphylococcus aureus = S. aureus*) and Gram-negative bacteria (*Escherichia coli = E. coli*) bacteria [45]. Subsequently, they continued to experiment with the same composites using the pulse ablation technique. Silver and copper nanoparticles were embedded into GO thin films using the laser ablation technique and tested against *E. coli* and *S. aureus*. The experiment concluded that the inhibition zone was 10.2 ± 1.1 mm against *E. coli* and 15.2 ± 1.6 mm against *S. aureus* [46]. In addition to silver, metallic zinc and zinc oxide particles have antibacterial properties. Considering the enhanced antibacterial effects described earlier, the addition of metallic oxides and metallic oxide nanoparticles to the GO sheets improved the antibacterial activity. Additionally, ZnO nanoparticles have shown good antibacterial activity when bacteria encounter ZnO ions along with disruption of the cell wall.

References

1. Bijesh, P.; Selvaraj, V.; Andal, V. A review on synthesis and applications of nano metal Oxide/porous carbon composite. Mater. Today Proc. 2021, 55, 212–219.
2. Li, F.; Jiang, X.; Zhao, J.; Zhang, S. Graphene oxide: A promising nanomaterial for energy and environmental applications. Nano Energy 2015, 16, 488–515.
3. Carolin, C.F.; Kumar, P.S.; Saravanan, A.; Joshiba, G.J.; Naushad, M. Efficient techniques for the removal of toxic heavy metals from aquatic environment: A review. J. Environ. Chem. Eng. 2017, 5, 2782–2799.
4. Wang, B.; Zhang, F.; He, S.; Huang, F.; Peng, Z. Adsorption Behaviour of Reduced Graphene Oxide for Removal of Heavy Metal Ions. Asian J. Chem. 2014, 26, 4901–4906.
5. Su, H.; Ye, Z.; Hmidi, N. High-performance iron oxide–graphene oxide nanocomposite adsorbents for arsenic removal. Colloids Surf. A Physicochem. Eng. Asp. 2017, 522, 161–172.

6. Fathy, M.; Moghny, T.A.; Mousa, M.A.; Abdou, M.M.; El-Bellihi, A.-H.A.-A.; Awadallah, A.E. Correction to: Absorption of calcium ions on oxidized graphene sheets and study its dynamic behavior by kinetic and isothermal models. Appl. Nanosci. 2018, 8, 2105.
7. Wang, J.; Chen, B. Adsorption and coadsorption of organic pollutants and a heavy metal by graphene oxide and reduced graphene materials. Chem. Eng. J. 2015, 281, 379–388.
8. Huang, H.; Wang, Y.; Zhang, Y.; Niu, Z.; Li, X. Amino-functionalized graphene oxide for Cr(VI), Cu(II), Pb(II) and Cd(II) removal from industrial wastewater. Open Chem. 2020, 18, 97–107.
9. Wan, S.; He, F.; Wu, J.; Wan, W.; Gu, Y.; Gao, B. Rapid and highly selective removal of lead from water using graphene oxide-hydrated manganese oxide nanocomposites. J. Hazard. Mater. 2016, 314, 32–40.
10. Naeem, H.; Ajmal, M.; Qureshi, R.B.; Muntha, S.T.; Farooq, M.; Siddiq, M. Facile synthesis of graphene oxide–silver nanocomposite for decontamination of water from multiple pollutants by adsorption, catalysis and antibacterial activity. J. Environ. Manag. 2018, 230, 199–211.
11. Lotfi, Z.; Mousavi, H.Z.; Sajjadi, S.M. Covalently bonded double-charged ionic liquid on magnetic graphene oxide as a novel, efficient, magnetically separable and reusable sorbent for extraction of heavy metals from medicine capsules. RSC Adv. 2016, 6, 90360–90370.
12. Dong, Y.; Wang, L.; Wang, J.; Wang, S.; Wang, Y.; Jin, D.; Chen, P.; Du, W.; Zhang, L.; Liu, B.-F. Graphene-Based Helical Micromotors Constructed by “Microscale Liquid Rope-Coil Effect” with Microfluidics. ACS Nano 2020, 14, 16600–16613.
13. Peng, W.; Li, H.; Liu, Y.; Song, S. A review on heavy metal ions adsorption from water by graphene oxide and its composites. J. Mol. Liq. 2017, 230, 496–504.
14. Archana, S.; Jayanna, B.; Ananda, A.; Shilpa, B.M.; Pandiarajan, D.; Muralidhara, H.; Kumar, K.Y. Synthesis of nickel oxide grafted graphene oxide nanocomposites—A systematic research on chemisorption of heavy metal ions and its antibacterial activity. Environ. Nanotechnol. Monit. Manag. 2021, 16, 100486.
15. Fu, Y.; Wang, J.; Liu, Q.; Zeng, H. Water-dispersible magnetic nanoparticle–graphene oxide composites for selenium removal. Carbon 2014, 77, 710–721.
16. Liu, Z.; Wang, Y.; Zhang, G.; Yang, J.; Liu, S. Preparation of graphene-based catalysts and combined DBD reactor for VOC degradation. Environ. Sci. Pollut. Res. 2022, 29, 51717–51731.
17. Yu, L.; Wang, L.; Xu, W.; Chen, L.; Fu, M.; Wu, J.; Ye, D. Adsorption of VOCs on reduced graphene oxide. J. Environ. Sci. 2018, 67, 171–178.
18. Shrivastava, S.; Thomas, S.; Sobhan, C.; Peterson, G. An experimental investigation of the CO2 adsorption performance of graphene oxide forms. Int. J. Refrig. 2018, 96, 179–190.

19. Vijay, S.; Ju, W.; Brückner, S.; Tsang, S.-C.; Strasser, P.; Chan, K. Unified mechanistic understanding of CO2 reduction to CO on transition metal and single atom catalysts. Nat. Catal. 2021, 4, 1024–1031.
20. Alves, D.C.B.; Silva, R.; Voiry, D.; Asefa, T.; Chhowalla, M. Copper nanoparticles stabilized by reduced graphene oxide for CO2 reduction reaction. Mater. Renew. Sustain. Energy 2015, 4, 2.
21. Xu, D.; Cheng, B.; Wang, W.; Jiang, C.; Yu, J. Ag2CrO4/g-C3N4/graphene oxide ternary nanocomposite Z-scheme photocatalyst with enhanced CO2 reduction activity. Appl. Catal. B Environ. 2018, 231, 368–380.
22. Habisreutinger, S.N.; Schmidt-Mende, L.; Stolarczyk, J.K. Photocatalytic Reduction of CO2 on TiO2 and Other Semiconductors. Angew. Chem. Int. Ed. 2013, 52, 7372–7408.
23. Rambabu, Y.; Kumar, U.; Singhal, N.; Kaushal, M.; Jaiswal, M.; Jain, S.L.; Roy, S.C. Photocatalytic reduction of carbon dioxide using graphene oxide wrapped TiO2 nanotubes. Appl. Surf. Sci. 2019, 485, 48–55.
24. Shown, I.; Hsu, H.-C.; Chang, Y.-C.; Lin, C.-H.; Roy, P.K.; Ganguly, A.; Wang, C.-H.; Chang, J.-K.; Wu, C.-I.; Chen, L.-C.; et al. Highly Efficient Visible Light Photocatalytic Reduction of CO2 to Hydrocarbon Fuels by Cu-Nanoparticle Decorated Graphene Oxide. Nano Lett. 2014, 14, 6097–6103.
25. Zhu, Z.; Han, Y.; Chen, C.; Ding, Z.; Long, J.; Hou, Y. Reduced Graphene Oxide-Cadmium Sulfide Nanorods Decorated with Silver Nanoparticles for Efficient Photocatalytic Reduction Carbon Dioxide Under Visible Light. ChemCatChem 2018, 10, 1627–1634.
26. Deerattrakul, V.; Dittanet, P.; Sawangphruk, M.; Kongkachuichay, P. CO2 hydrogenation to methanol using Cu-Zn catalyst supported on reduced graphene oxide nanosheets. J. CO2 Util. 2016, 16, 104–113.
27. Yue, T.; Huang, H.; Chang, Y.; Jia, J.; Jia, M. Controlled assembly of nitrogen-doped iron carbide nanoparticles on reduced graphene oxide for electrochemical reduction of carbon dioxide to syngas. J. Colloid Interface Sci. 2021, 601, 877–885.
28. Zhang, Z.; Ahmad, F.; Zhao, W.; Yan, W.; Zhang, W.; Huang, H.; Ma, C.; Zeng, J. Enhanced Electrocatalytic Reduction of CO2 via Chemical Coupling between Indium Oxide and Reduced Graphene Oxide. Nano Lett. 2019, 19, 4029–4034.
29. Saquib, M.; Halder, A. Reduced graphene oxide supported gold nanoparticles for electrocatalytic reduction of carbon dioxide. J. Nanopart. Res. 2018, 20, 46.
30. Wu, D.; Chen, W.; Wang, X.; Fu, X.-Z.; Luo, J.-L. Metal-support interaction enhanced electrochemical reduction of CO2 to formate between graphene and Bi nanoparticles. J. CO2 Util. 2020, 37, 353–359.

31. Xi, J.; Li, Y.; Zhou, E.; Liu, Y.; Gao, W.; Guo, Y.; Ying, J.; Chen, Z.; Chen, G.; Gao, C. Graphene aerogel films with expansion enhancement effect of high-performance electromagnetic interference shielding. Carbon 2018, 135, 44–51.
32. Xu, L.; Zhang, W.; Wang, L.; Xue, J.; Hou, S. Large-scale preparation of graphene oxide film and its application for electromagnetic interference shielding. RSC Adv. 2021, 11, 33302–33308.
33. Shi, K.; Su, J.; Liang, H.; Hu, K.; Xu, J. Highly optically transparent graphene mesh for electromagnetic interference shielding. Diam. Relat. Mater. 2022, 123, 108849.
34. Ghosh, K.; Srivastava, S.K. Enhanced Supercapacitor Performance and Electromagnetic Interference Shielding Effectiveness of CuS Quantum Dots Grown on Reduced Graphene Oxide Sheets. ACS Omega 2021, 6, 4582–4596.
35. Li, J.; Huang, L.; Yuan, Y.; Li, Y.; He, X. Mechanically strong, thermally conductive and flexible graphene composite paper for exceptional electromagnetic interference shielding. Mater. Sci. Eng. B 2020, 263, 114893.
36. Kumar, P.; Shahzad, F.; Hong, S.M.; Koo, C.M. A flexible sandwich graphene/silver nanowires/graphene thin film for high-performance electromagnetic interference shielding. RSC Adv. 2016, 6, 101283–101287.
37. Fu, P.; Huan, X.; Luo, J.; Ren, S.; Jia, X.; Yang, X. Magnetically Aligned Fe3O4 Nanowires-Reduced Graphene Oxide for Gas Barrier, Microwave Absorption, and EMI Shielding. ACS Appl. Nano Mater. 2020, 3, 9340–9355.
38. Qu, Z.; Wang, Y.; Wang, W.; Yu, D. Robust magnetic and electromagnetic wave absorption performance of reduced graphene oxide loaded magnetic metal nanoparticle composites. Adv. Powder Technol. 2020, 32, 194–203.
39. Torrisi, L.; Silipigni, L.; Cutroneo, M. Graphene oxide as a radiation sensitive material for XPS dosimetry. Vacuum 2020, 173, 109175.
40. Silipigni, L.; Cutroneo, M.; Salvato, G.; Torrisi, L. In-situ soft X-ray effects on graphene oxide films. Radiat. Eff. Defects Solids 2018, 173, 740–750.
41. Malinský, P.; Macková, A.; Florianová, M.; Cutroneo, M.; Hnatowicz, V.; Boháčová, M.; Szőkölová, K.; Böttger, R.; Sofer, Z. The Structural and Compositional Changes of Graphene Oxide Induced by Irradiation With 500 keV Helium and Gallium Ions. Phys. Status Solidi (b) 2018, 256, 1800409.
42. Malinský, P.; Cutroneo, M.; Sofer, Z.; Szőkölová, K.; Böttger, R.; Akhmadaliev, S.; Macková, A. Structural and compositional modification of graphene oxide by means of medium and heavy ion implantation. Nucl. Instrum. Methods Phys. Res. Sect. B Beam Interact. Mater. At. 2019, 460, 201–208.

43. Neto, S.M.; Almeida, K.C.D.; Macedo, M.L.R.; Franco, O.L. Understanding bacterial resistance to antimicrobial peptides: From the surface to deep inside. Biochim. Biophys. Acta (BBA) -Mol. Cell Res. 2015, 1848 Pt B, 3078–3088.
44. Rodríguez-Otamendi, D.I.; Meza-Laguna, V.; Acosta, D.; Álvarez-Zauco, E.; Huerta, L.; Basiuk, V.A.; Basiuk, E.V. Eco-friendly synthesis of graphene oxidesilver nanoparticles hybrids: The effect of amine derivatization. Diam. Relat. Mater. 2021, 111, 108208.
45. Menazea, A.; Ahmed, M. Synthesis and antibacterial activity of graphene oxide decorated by silver and copper oxide nanoparticles. J. Mol. Struct. 2020, 1218, 128536.
46. Menazea, A.; Ahmed, M. Silver and copper oxide nanoparticles-decorated graphene oxide via pulsed laser ablation technique: Preparation, characterization, and photoactivated antibacterial activity. Nano-Struct. Nano-Objects 2020, 22, 100464.